Journal of Orthopaedic Research®

Check for updates

RESEARCH ARTICLE OPEN ACCESS

Characterizing Microstructural and Mechanical Properties of Dancer Achilles Tendon Using Ultrashort Echo Time MRI and Shear Wave Elastography Ultrasound

Anna M. Horner[1] | Felix M. Gonzalez[2,3] | Courtney N. Gleason[1,4] | Amanda Blackmon[5,6] | Emma Faulkner[5,7] | Damian Dyckman[2] | Monica B. Umpierrez[2] | Philip K.-W. Wong[2] | Vahid Khalilzad Sharghi[8] | Pan Su[9] | David A. Reiter[2,4,10]

[1]School of Medicine, Emory University, Atlanta, USA | [2]Department of Radiology and Imaging Sciences, Emory University, Atlanta, USA | [3]AdventHealth Radiology Central Florida, Orlando, USA | [4]Department of Orthopedics, Emory University, Atlanta, USA | [5]Atlanta Dance Medicine, Roswell, USA | [6]Physical Therapy, Mercer University, College of Health Professions, Macon, USA | [7]Dance Program, Department of Theater and Dance, Emory University, Atlanta, USA | [8]Siemens Healthineers, Atlanta, USA | [9]Siemens Medical Solutions USA Inc., Malvern, USA | [10]Biomedical Engineering Department, Emory University and Georgia Technological Institute, Atlanta, USA

Correspondence: David A. Reiter (dareite@emory.edu)

Received: 24 March 2025 | **Revised:** 7 September 2025 | **Accepted:** 14 September 2025

Funding: This study was supported in part by an Emory Orthopedics Research Pilot Grant, Emory Radiology and Imaging Sciences Pilot Grant, and National Institutes of Health (NIH) R21AR080869.

Keywords: Achilles tendon | multi-echo ultrashort echo time (UTE) magnetic resonance imaging (MRI) | performing arts | shear wave elastography | sports medicine | tendon stiffness

ABSTRACT

Previous observations of multi-echo ultrashort echo time (UTE) magnetic resonance imaging (MRI) decay data from the Achilles tendon (AT) report an off-resonance non-water signal associated with non-collagenous extracellular matrix (ECM) constituents. This cross-sectional study investigates the relationship between this MRI-derived tissue matrix signal and mechanical stiffness of the AT in professional ballet dancers and non-dancer adults. Multiexponential analysis of multi-echo UTE MRI was used to quantify water components and an off-resonance AT matrix component. To compare AT structure with its functionality, shear wave elastography (SWE) ultrasound US was used to measure tendon stiffness along both longitudinal (V_L) and transverse (V_S) axes. 34 participants, including 15 ballet dancers and 19 non-dancers, were studied. Dancers exhibited significantly larger V_S ($p = 0.013$) compared to non-dancers, consistent with prior observations of a training effect in tendon from repeated loading with exercise. UTE-derived off-resonance relaxation component amplitude, β_3, was positively associated with V_L in dancers ($p = 0.029$) and V_S in non-dancers ($p = 0.024$), suggesting a microstructural role of this matrix component. While additional work is needed to unambiguously assign this off-resonance signal, these findings suggest its association with non-collagenous ECM and show potential for combined use of UTE and SWE imaging to assess tendon structure-function relationships and adaptations to mechanical loading in vivo.

1 | Introduction

The Achilles tendon (AT) plays an important role in transmitting forces between the muscles and bones responsible for human ambulation and athletic movements (dancing, balance, jumping) [1, 2]. Tendon composition consists of primarily water (50%–75%) and extracellular matrix (ECM) with low cellularity. ECM is primarily type 1 collagen (60%–85% dry mass), which has traditionally been thought to provide the majority of tensile strength to the tendon [3, 4]. Relative to type 1 collagen, investigation of non-collagenous matrix constituents such as proteoglycans, elastin, and cartilage oligomeric matrix protein (COMP) have previously been ignored. However, recent work demonstrates the importance of non-collagenous matrix constituents in the modulation of tendon mechanical properties [5–7]. Mechanical function of tendons is influenced by both the water distribution within the tissue compartments and its matrix composition [3, 8, 9]. Remodeling of tendon composition and microstructure are influenced by repeated mechanical stimulation. This remodeling can lead to either adaptive modifications that increase tendon stiffness or maladaptive changes leading to tendinopathy [10, 11].

Multi-echo ultrashort echo time (UTE) magnetic resonance imaging (MRI) provides noninvasive and quantitative information on both tendon matrix constituents and water distribution within the tendon matrix. Conventionally, a two compartment model has been proposed to quantify water bound to collagen molecules and free water in the surrounding extracellular matrix (ECM), using the UTE MRI water relaxation signal. We have recently extended this relaxation modeling approach to additionally allow for characterization of a non-water compartment attributed to the extracellular matrix (Figure 1). In our previous work, we observed an off-resonance UTE signal with a frequency consistent with glycosylated ECM proteins [12]. The interpretation of this additional off-resonance signal has been supported using detailed nuclear magnetic resonance (NMR) studies to assign its origin to non-collagenous ECM components [12, 13]. Currently, the origin of this off-resonance UTE chemical shift has not been definitively assigned and its relationship to functional properties of tendon have not been established.

Shear wave elastography (SWE) ultrasound (US) provides noninvasive and reliable quantification of AT stiffness properties [14, 15]. Shear wave speed (V, in m/s) represents tissue stiffness and is measured with SWE. In other US applications, such as body imaging of the liver, shear modulus is often

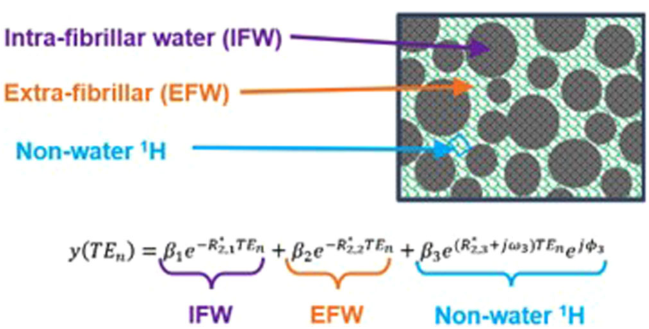

FIGURE 1 | Structural schematic of tendon microstructure, with water and non-water proton matrix pools accounted for by our multi-exponential model. β_1 represents the collagen-bound water, β_2 represents the free water in the tendon, and the non-water matrix pool is represented as a single, off-resonant component denoted β_3. As such, β_1 and β_2 are reported as a relative ratio to $\beta_1 + \beta_2$ while β_3 is reported as a ratio to $\beta_1 + \beta_2 + \beta_3$.

computed from shear wave speed (μ, in kPa) with the equation:

$$\mu = \rho \times V^2$$

where ρ represents tissue density (approximately 1000 kg/m^3 in the human body) [16]. It is important to note that this shear modulus calculation relies on two assumptions: the tissue is homogenous with a known density and it displays linear elasticity, meaning the strain of the tissue is directly proportional to the force applied to it. For this musculoskeletal application, we focus on shear wave speed to avoid misinterpretations potentially resulting from discrepancies between the ideal tissue characteristics in these assumptions and the measured tissue since tendon is heterogenous and displays anisotropic properties in addition to linear elasticity.

Prior studies have demonstrated that shear waves spread differently depending on tissue characteristics, such as tendon loading, axis orientation, or presence of tendinopathy. Generally, waves propagate faster in loaded tendons, slower along the short axis of healthy tendons compared to the long axis, and slower in tendinopathic tendons [17–20]. The AT of jumping athletes (i.e., ballet dancers) display distinguishable structural adaptations compared to control AT, presumably to withstand a high frequency of mechanical loading [21]. Interestingly, the intensive training of professional ballet dancers results in detectable changes in the ultrasound tendon characteristics of Achilles tendon as early as 6 weeks [22]. SWE US has detected increased stiffness in ballet dancer AT compared to both runners and non-running athletes of similar age [23]. Due to the specialized conditioning of dancer AT, we suspect that detection of structure-function interplay would be plausible in this specific group of athletes. Given factors that influence tendon remodeling, comparison with a population of older non-dancer adults could provide additional insight into Achilles tendon structure-function as assessed using SWE and UTE.

We hypothesize that the variation in mechanical stiffness of tendon is associated with ECM composition, both of which are influenced by multiple factors-including age and the amplitude and frequency of daily tendon loading-and observable using SWE and UTE. This study first reports the SWE-derived mechanical properties and UTE-derived composition and relaxation properties of healthy AT between professional ballet dancers and older non-dancer adults. These two groups represent a wide range of factors expected to influence both mechanical and compositional tendon properties. Subsequently, relationships between the off-resonance UTE-derived ECM component and SWE-derived tissue mechanical properties are analyzed in both professional ballet dancers and older non-dancer adults. Additionally, relationships between the UTE off-resonance ECM component and UTE-derived water compartmentation in the AT are analyzed. Insights into tendon structure-function relationships and in vivo adaptations to mechanical loading provide the potential for improved assessment of tendon health. This enhanced understanding of tendon matrix properties could also inform injury prevention or rehabilitation strategies in the clinical setting.

2 | Methods

2.1 | Subjects and Experimental Design

This prospective IRB-approved study recruited healthy, asymptomatic professional ballet dancers and healthy, asymptomatic non-dancer adults. Ballet dancers were assessed at the beginning of their training season under the supervision of company physical therapists. Dancer SWE and UTE MRI data acquisition occurred in the fall of 2022 and has not been previously described, though there may be some subjects that overlap with [23]. Descriptive results of UTE MRI data from $n = 6$ non-dancer subjects have been reported previously in [12].

2.2 | Inclusion Criteria and Categorization

This study included both healthy non-dancer and professional ballet dancer adults who were able to provide written and verbal informed consent to participate with sonographic and magnetic resonance imaging of their ankles. All subjects were able to ambulate voluntarily with no limitations. They also had minimal to no symptoms or complaints relating to their AT or ankle at rest or during physical activity.

Initial survey questions were conducted to collect demographic information (such as age, BMI, height, and activity level) as well as screening for exclusion criteria. Ankle activity level was defined using a 0 to 10 grade scale to produce a cumulative score based on an individual's self-reported physical capability, as described in [24]. Ankle dominance was assigned based on subjects' answers to survey questions (i.e., handedness, preference for kicking a ball, lead jumping leg).

2.3 | Exclusion Criteria

Participants with any personal history of ankle surgery, pathology that affected AT quality (gout, ankylosing spondylitis, reactive arthritis, fluoroquinolone-associated tendinopathy, psoriasis, Reiter syndrome, or any other rheumatologic or hypercholesteremic condition) were excluded from this study. A subject with AT pathology or tendinopathy from any insult within the past 6 months were also excluded (including from operative repair, trauma, athletic participation, or tendon pain). Finally, any presence of skin lesions, abrasions, or lacerations located in the imaged body area were also excluded. These exclusion criteria were replicated from [23].

Due to image quality concerns of the UTE MRI portion of the study, one dancer was excluded from the study post data acquisition but before data analysis. We do not count this participant toward our sample size.

2.4 | Ultrasound and Shear Wave Elastography

AT assessment was performed by a fellowship-trained musculoskeletal (MSK) radiologist using a 2D SWE instrument (Logiq S8 US machine; GE Healthcare, Little Chalfont, UK). Measurements were performed with the ankle in voluntary active maximum dorsiflexion (DF). Study participants were positioned lying prone with their feet over the edge of the examination table. The 9 L-D, 5- to 15-MHz linear array transducer was positioned parallel to the long axis of the AT to allow measurement of the entire tendon length in grayscale B-mode (Figure 2) using a panoramic image capture [25, 26]. After tendon length was measured, the probe was rotated 90° to determine the largest dimension in both width and the antero-posterior direction of the short axis, which was deemed the “mid-substance” of the AT. Once identified, the same US machine was changed to elastography mode and a 20-mm-thick gel standoff pad (Aquaflex; Parker Laboratories, Fairfield, NJ) was placed between the transducer and the subject's skin, according to the manufacturer's recommendations for musculoskeletal applications of SWE. All elastography measurements were made at the visualized mid-substance of the Achilles tendon, approximately 5 cm superior to its insertion on the calcaneus, of the subject's dominant ankle in both the transverse and longitudinal planes. To ensure optimal measurements and avoid outlying readings from applied

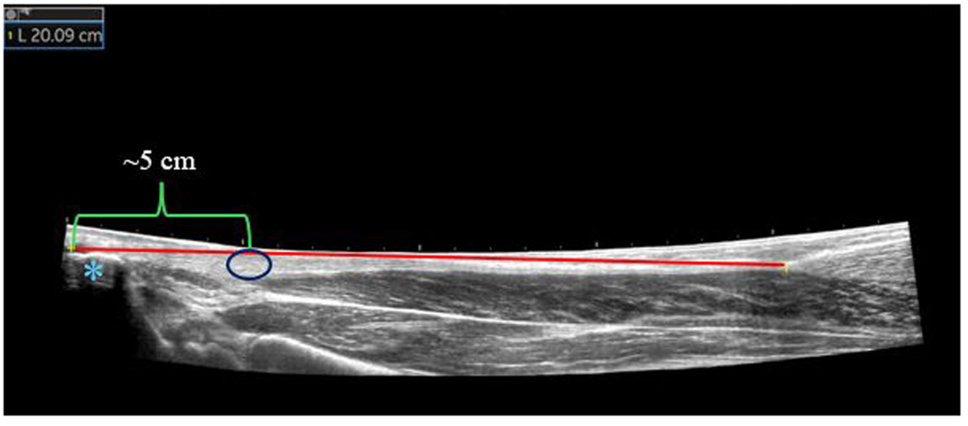

FIGURE 2 | Representation of panoramic imaging of the Achilles tendon (AT) in the long axis with red line denoting the tendon length (as starting from its insertion onto the calcaneus on the left to medial gastrocnemius muscle tendon junction on the right), blue * denoting the calcaneus, the green brackets denoting a distance of 5 cm as measured by the ultrasound machine, and the dark blue circle denoting the visualized midsubstance of the AT.

pressure probe variations, elastography maps were qualitatively evaluated for homogeneity throughout the entire examination [23, 27]. Shear stiffness was recorded using wave velocity (m/s) with measurements made along the short axis (V_S) and long axis (V_L) relative to the AT (Figure 3), as previously described in [25], using a region of interest defined within the image [25]. The US machine and probe can reliably measure tendon shear wave speed up to 15 m/s and this technique was further validated in [27] by using three musculoskeletal radiologists making repeated SWE measurements on the same subjects AT with excellent interobserver reliability and agreement [27]. For this study, a single image taken by one operator was used for all AT measurements throughout the entire US exam.

2.5 | MRI

MRI was performed at 3 T (MAGNETOM Prisma Fit; Siemens Healthineers, Forchheim, Germany) using a 4-channel radio frequency coil, wrapped around the posterior part of the study participant's dominant ankle. Subjects were positioned lying supine and feet first with adequate padding for comfort and secured to the exam table with positioning straps to minimize exam motion during image acquisition. Multi-echo UTE images were acquired using a prototype 3D stack-of-spirals research sequence with 16 echoes ranging from a minimum echo time of 60 μs to a maximum echo time of 30 ms. Echo times were sampled with nonlinear spacing to allow digitization of water and chemically shifted protons from the matrix. Additional sequence parameters included 40 ms repetition time, 30-degree excitation flip angle, 4 mm out of plane resolution and 0.625 mm in plane resolution, scan time is approximately 45 min.

2.6 | MRI Analysis

Regions of interest were selected in the UTE image at the visualized mid-substance of the AT and approximately 5 cm superior to its insertion on the calcaneus in an effort to match the location of SWE tendon stiffness measurements (Figure 4). In lieu of the conventional bi-exponential model that only

FIGURE 4 | Representative region of interest shown in the sagittal plane of a UTE image (TE = 3.8 ms) selected at the mid-substance of the human AT for relaxation signal quantification.

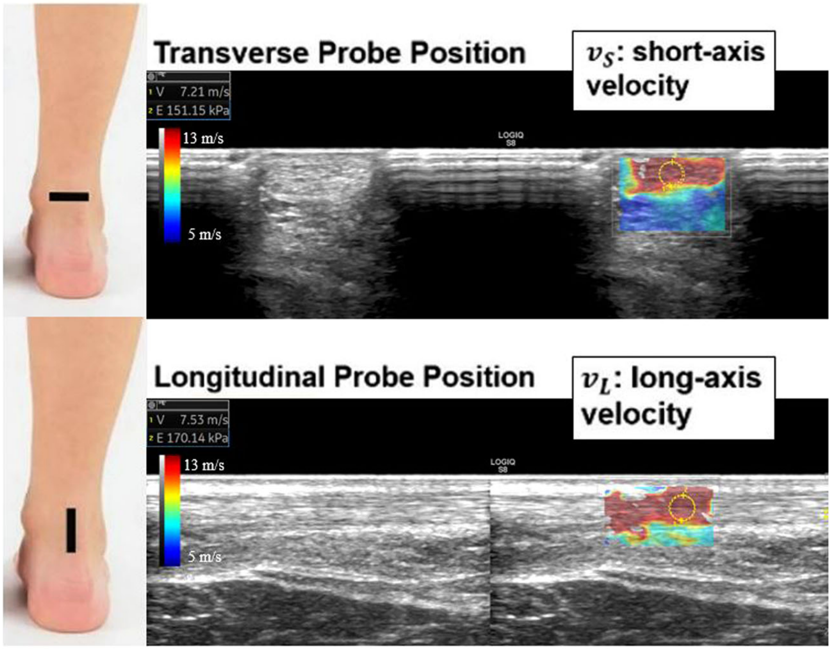

FIGURE 3 | Representative SWE US probe orientation on the AT (depicted with black bar) showing measurements in the transverse and longitudinal orientations captured at approximately 5 cm proximal to the distal insertion of the calcaneus. Shear wave maps were obtained in the axial (transverse) and sagittal (longitudinal) planes with colorimetric scale ranging from 5 to 13 m/s.

captures water proton pools, multi-exponential fitting of the UTE relaxation signals was performed:

$$y(TE_n) = \beta_1 e^{-R^*_{2,1}TE_n} + \beta_2 e^{-R^*_{2,2}TE_n} + \beta_3 e^{(R^*_{2,3}+j\omega_3)TE_n} e^{j\phi_3}$$

where β_k, $R^*_{2,k}$, ω_k and ϕ_k represent the amplitude fraction ($\sum\beta_k = 1$), relaxation rate, frequency, and phase of the k-th component, respectively. Signals from on-resonance relaxation components, represented as β_1 and β_2, have been previously attributed to rapidly relaxing collagen-bound water and more slowly relaxing interstitial water, respectively [9]. The current model (Figure 1) includes an off-resonance relaxation component (β_3) that has previously been attributed to protons chemically shifted from water that reside within the extracellular matrix [12]. As such, β_1 and β_2 are reported as a relative ratio to $\beta_1 + \beta_2$ while β_3 is reported as a ratio to $\beta_1 + \beta_2 + \beta_3$.

2.7 | Statistics

Demographic characteristics were summarized using means and standard deviations for continuous variables. Two-tailed t-tests were performed to determine if differences in SWE and UTE parameters between professional ballet dancers and non-dancer adults. Due to the limited sample size, comparisons were limited to the specific subset of SWE and UTE parameters needed to test the hypothesis above: V_L, V_S, β_2, and β_3. β_1 was omitted due to its numerical dependence on β_2. Pearson correlation was performed to examine if linear relationships existed between microstructure UTE and mechanical SWE properties. The Benjamini-Hochberg method was used for group-wise and correlation analyses to decrease the probability of false-positives from multiple comparisons, with a false-discovery rate of $\alpha = 0.1$.

3 | Results

34 total participants were enrolled and evaluated in this study including 19 healthy, non-dancer adults and 15 professional ballet dancers. Data from one ballet dancer was excluded based on insufficient UTE image quality ($n = 33$). Table 1 shows subject characteristics of dancer and non-dancer groups. Dancers were younger with lower weight and BMI than non-dancers.

Table 2 shows SWE and UTE parameter averages and standard deviations for the subset of tendon properties compared between the dancer and non-dancer groups (complete list of parameters shown in Table S1). SWE showed larger V_S ($p = 0.013$) in dancers. All multi-echo UTE MRI signal decays exhibited oscillations that were represented with minimal error using the three-component model (Figure 5). The frequency (ω_3) of the off-resonance component was 365 ± 82.5 Hz and 369 ± 137 Hz from the water signal for the non-dancer and dancer cohorts, respectively (see Table S1). There were no statistically significant group differences in UTE parameters, however the off-resonance signal amplitude trended lower in dancers ($p = 0.050$, Table 2).

TABLE 1 | Study subject characteristics by group.

Variable	Overall ($N = 33$)	Dancer	Non-dancer
Gender			
Male	18 (55%)	6 (43%)	12 (63%)
Female	15 (45%)	8 (57%)	7 (37%)
Age (years)	33.5 ± 12.2	23.9 ± 3.4	40.5 ± 12.0*
Body Mass Index (kg/m^2)	22.6 ± 3.7	20.0 ± 1.7	24.6 ± 3.5*
Height (m)	1.7 ± 0.1	1.7 ± 0.1	1.7 ± 0.1
Mass (kg)	66.6 ± 15.0	57.2 ± 10.9	73.5 ± 13.9*

*Indicates a difference with $p < 0.05$ between dancer and non-dancer groups.

TABLE 2 | UTE and SWE measurements showing group differences in ECM/water distribution and mechanical properties of AT by group. All values reported as mean ± standard deviation unless otherwise noted. β_2 represents the slowly relaxing water component, β_3 the off-resonant ECM component, V_L the long axis shear wave velocity, and V_S the short axis shear wave velocity of AT.

Variable	Non-dancer	Dancer
UTE		
β_2	0.178 ± 0.058	0.147 ± 0.077
β_3	0.156 ± 0.070	0.113 ± 0.052(*)
SWE		
V_L (m/s)	7.868 ± 0.424	7.799 ± 0.650
V_S (m/s)	7.237 ± 0.422	7.743 ± 0.607*

*Indicates a statistically significant difference between groups based on the Benjamini–Hochberg method using a false discovery rate of $\alpha = 0.1$.
(*) Indicates a mean difference between groups with $p = 0.05$.

Within-group correlations between SWE and UTE parameters were analyzed to assess relationships between tendon microstructure and function. In the ballet dancers, off-resonance component amplitude, β_3 was directly correlated with tendon longitudinal SWE velocity V_L ($\rho = 0.58$, $p = 0.029$, Figure 6A). In the non-dancer group, β_3 was directly correlated with the short axis SWE velocity, V_S ($\rho = 0.52$, $p = 0.024$, Figure 6B). Additionally, there was a positive association between β_3 and β_2 ($\rho = 0.50$, $p = 0.031$, Figure 6C) in non-dancers, suggesting increased concentration of this off-resonance ECM component (represented by β_3) is associated with an increased proportion of unbound bulk water (represented by β_2) in the tendon (see Figure 1).

4 | Discussion

This study suggests that applying the multi-component UTE model used in this study provides a link between tendon ECM components and mechanical adaptations from sport, potentially providing a framework for understanding tendon injury and treatment response. SWE US tendon stiffness has been investigated before this study and shown to be reliable in

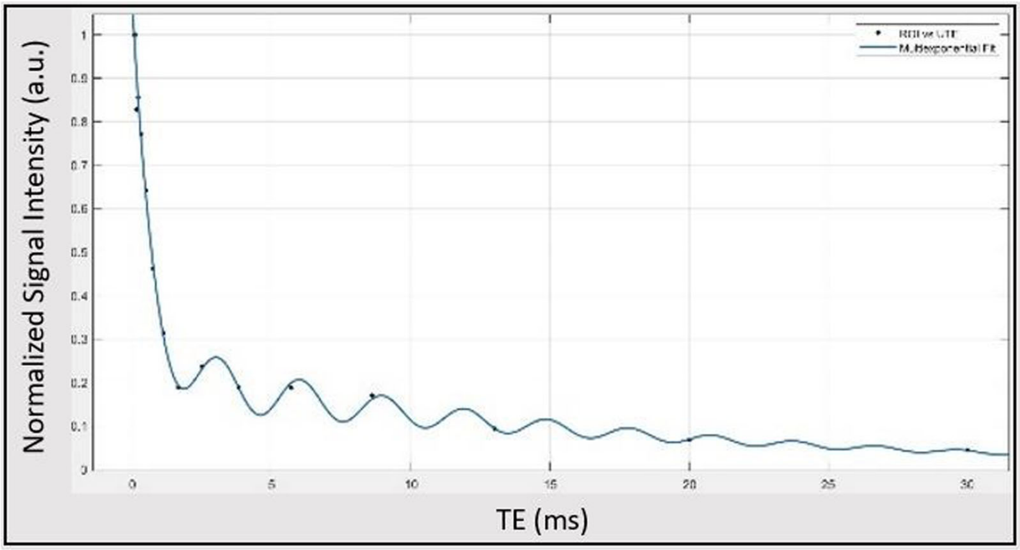

FIGURE 5 | Representative multi-echo UTE decay signal from the AT mid-substance ROI with multiexponential fit overlayed to demonstrate the appropriateness of our multi-component model.

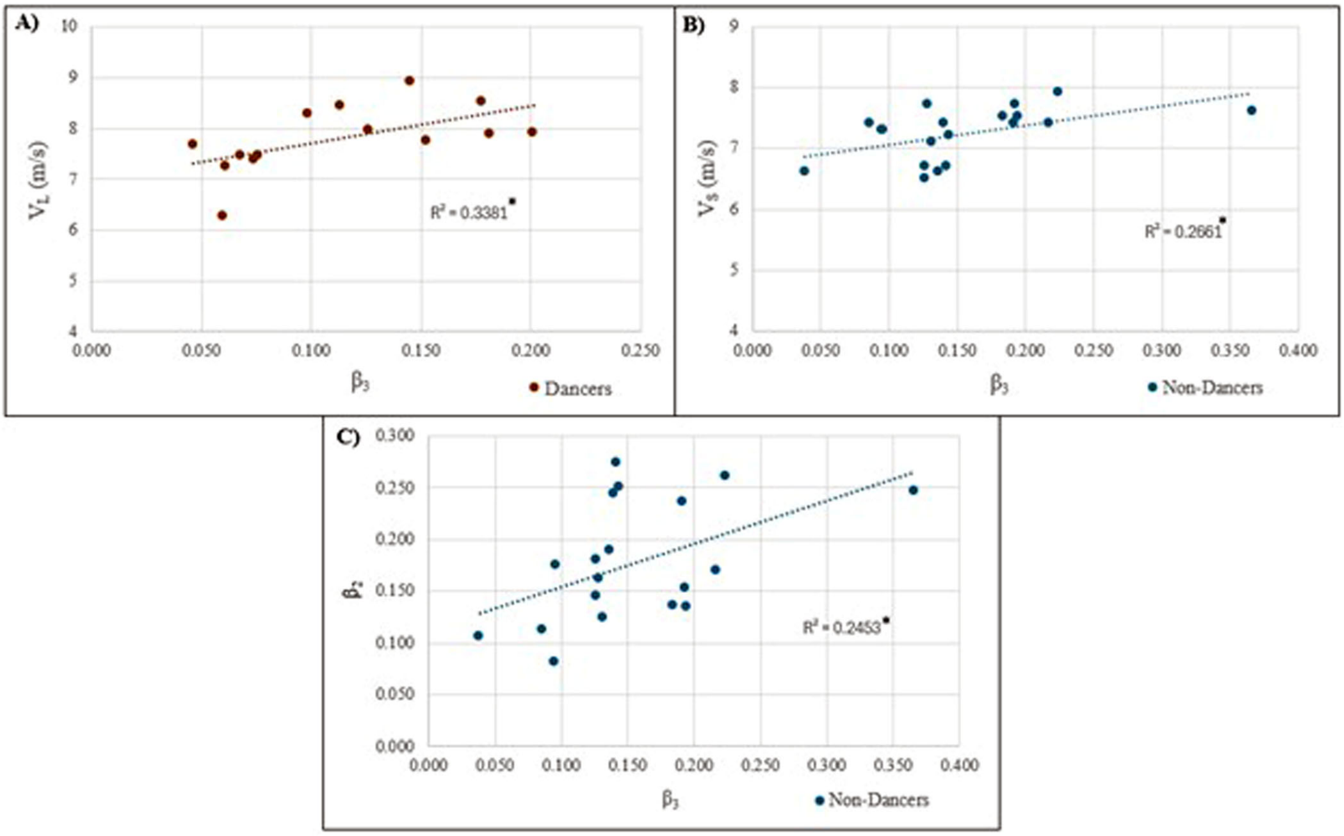

FIGURE 6 | SWE and UTE correlations among non-dancers and professional dancers. (A) Positive association ($p = 0.029$) was observed between off-resonance signal amplitude (β_3) and SWE wave speed in the longitudinal direction (V_L), reflecting an increase in stiffness with increasing amplitude of matrix pool. (B) Positive association ($p = 0.024$) between non-dancer signal amplitude (β_3) and SWE wave speed in the transverse direction (V_S), reflecting an increase in stiffness with increasing amplitude of matrix pool. (C) Exploratory analysis revealed a positive association ($p = 0.031$) between signal amplitude (β_3) and long component (β_2), suggesting increases in this ECM component is associated with an increase in the free water pool size in non-dancers.

determining injured versus non-injured states. Healthier tendons exhibit greater stiffness while "softness" is associated with tendinopathies and self-reported clinical symptoms [17, 18]. Regarding our SWE measurements, we found increased V_S in dancers compared to older non-dancers, similar to the stiffer V_S in dancers compared to runners and non-athletes reported in [23]. However, there was no significant difference in V_L between dancers versus non-dancers, while [23] reported higher V_L in the dancer group. Collagen fibrils in tendons are orientated in the longitudinal direction while supporting proteins, such as ECM proteins, are intermixed throughout the tendon structure with various interactions with each other and collagen fibrils (transverse, longitudinal, oblique, multi-directional axes). Thus, greater short axis stiffness may indicate structural reinforcement of the support proteins rather than collagen fibrils, whereas long axis stiffness could be due to changes in collagen fiber properties. We note that our nondancer group in the current study is significantly older so this discrepancy could be due to an age effect.

With the development of multi-echo UTE MRI, we are now able to observe more detailed tendon microstructure in vivo that was previously only detectable *ex vivo*. Interestingly, an off-resonance component unaccounted for by the standard bi-component model of tendon microstructure has been detected [12]. The tissue components giving rise to off-resonance signals in multi-echo UTE decay data from tendon have yet to be definitively assigned. High-resolution magic angle spinning (HRMAS) NMR studies of healthy and damaged tendon explant tissue have identified prominent resonances assigned to chemical groups belonging to ECM proteins, glycoproteins, and metabolites [13]. Importantly, HRMAS NMR captures an idealized representation of the chemical shift spectrum by leveraging high radiofrequency power, sample spinning, and magic angle position to provide high spectral resolution of semi-solid tissues. However, many of these spectral lines are broadened with conventional MRI acquisition, rendering them undetectable. With UTE, we consistently observe an off-resonance signal amplitude with an average chemical shift frequency comparable to glycoprotein subunits in tendon. The chemical shift frequencies observed in this study are consistent with our previous work in healthy non-athletic volunteers [12]. Similar chemical shift frequencies have been identified in the intervertebral disc using in vivo ^{1}H magnetic resonance (MR) spectroscopy and attributed to the N-acetal resonance in proteoglycan [28]. The fitted frequency value for this component in the dancer cohort showed a somewhat large variance among subjects, influenced by readings from 6 subjects showing offset frequencies greater than the mean value. In general, large variance in frequency estimation could be a result of the model, which only represents a single off-resonance component. If multiple MR-visible off-resonance components are present in tendon, fitting of a single off-resonance component can produce greater dispersion errors in frequency estimation [12]. Additionally, the use of nonlinear echo spacing can lead to reduced accuracy and precision of frequency estimation. Despite these limitations, multi-echo UTE signal decays from tendon consistently exhibit a detectable off-resonance signal amplitude.

The off-resonance signal amplitude (β_3) shows a direct association with SWE tendon stiffness measures in dancers and non-dancers, suggesting its association with a matrix constituent of structural origin. However, this structure-function relationship appears to exist for tendon stiffness measures in different orientations of the tendon: i.e., (β_3) is correlated with stiffness along the tendon in dancers and is correlated with stiffness perpendicular to the length of the tendon in non-dancers. Previous work demonstrates that non-collagenous ECM proteins serve a vital role in the tendon's mechanical properties, including load-bearing functionality in addition to the known role of type I collagen [3, 5–7, 10, 11, 29]. Among these ECM components are proteoglycans, elastin, and COMP, which all exhibit chemical shift resonances comparable to those reported here and serve as major constituents in pericellular and interfascicular matrices. These components also function in the viscoelastic responses to shear, tension, and compressive loading in both the fiber direction and orthogonal to the fiber direction [5–7]. For example, defective decorin and biglycan (the primary proteoglycans found in ECM of tendon) in mice knockouts have lower tendon stiffness measurements post-injury compared with wild-type mice [30]. Similarly, mutations in COMP result in joint laxity in humans, and both COMP and elastin knockout mice display an increased diameter of the collagen fibrils in their AT, which is assumed to be compensatory response [6, 31]. Indeed, several ECM components have been shown to facilitate collagen formation during matrix remodeling resulting in increased tensile stiffness [6, 32], consistent with our observed positive association between β_3 and V_L in dancers. In non-dancers, the positive association between β_3 and β_2 might suggest hydrophilic properties of this ECM component as would be expected in small leucine-rich proteoglycans (SLRPs), attracting water to the bulk water compartment. SLRPs are known to be attached and oriented laterally between collagen fibers [33] and thus could provide increased lateral stiffness, consistent with the observed direct correlation between β_3 and V_S in this group. Given the observed relationships between SWE-derived stiffness and the off-resonance component of our UTE model, we believe this UTE signal is related to these ECM proteins and could have some influence on the variation in AT mechanical properties.

The ability to non-invasively measure variation in tendon molecular composition and relate this to structural and functional changes is highly desirable and yet still somewhat elusive. UTE MRI combined with quantitative magnetization transfer (qMT) has shown sensitivity to pathomimetic treatment of tendon samples with collagenase [34]. However, this study primarily focused on degradation of type I collagen, lacking assessment of additional non-collagenous matrix components. Additionally, quantitative MR parameters have been nonspecifically attributed to varying amounts of collagen and glycosaminoglycans in cadaveric AT tissue samples at its enthesis site [35]. Our initial results suggest that the off-resonance UTE signal component may provide more direct quantitation on these non-collagen matrix components.

The utilization of noninvasive, nonradiative imaging modalities to assess tendon structure and function is advantageous. Comparing SWE parameters with corresponding UTE measurements could potentially capture information about tendon structure-function properties in vivo. Further development of this approach could be used to inform injury prevention or rehabilitation strategies.

There are some limitations of this study worth noting. Our small sample size, especially regarding the professional ballet dancer cohort ($n = 14$), likely limited our ability to compare SWE and UTE parameters. However, these initial comparisons suggest that there is sensitivity of these two modalities for structure-function studies in tendon and supports further evaluation in larger cohorts. The groups in this study were also not age-matched and therefore age-effects could influence differences in tendon composition and stiffness properties, especially given the significant age differences between the dancer and non-dancer groups. In addition to lower age, dancers also had lower BMIs when compared to the non-dancer group, introducing another potential confounder. We also note UTE and SWE observations from the professional dancers were obtained mid-season, so ongoing AT matrix remodeling is expected. Further work with longitudinal or age-matched cross-sectional observations of groups over a range of activity-level would be useful for directly assessing SWE US and UTE metrics of structure-function changes with activity. Finally, we note that in vivo measurement of tendon properties is affected by tendon loading and thus there has been debate in terms of best practices for reliable quantification of meaningful tendon stiffness properties (e.g. under neutral-relaxed, dorsiflexed, constant-applied ankle torque, static standing, etc.). We performed all shear wave measurements under voluntary maximum dorsiflexion in this study based on our prior observations that this ankle positioning produced the most reproducible measurements. We note that like all ankle positioning/loading protocols, this procedure could impart some influence on the measured stiffness properties.

5 | Conclusion

This study demonstrates associations between AT microstructural components and tendon stiffness as assessed by multiecho UTE MRI and SWE US, respectively, in professional ballet dancers and non-dancers. Increased tendon stiffness was associated with off-resonance UTE signal components, suggesting a structural origin of this off-resonance signal from non-collagenous extracellular matrix proteins that may play a critical role in tendon mechanical adaptations. These findings highlight the potential of integrating UTE and SWE imaging to investigate tendon structure-function relationships and adaptations to mechanical loading in vivo. Enhanced structure-function assessment of tendon health and injury status could improve rehabilitation protocols or injury prevention strategies for athletes, including professional dancers.

Author Contributions

Anna M. Horner: Performed image acquisition, data analysis, and manuscript writing. **Felix M. Gonzalez:** Principal investigator of Emory Radiology and Imaging Sciences Pilot grant. Performed logistical organization of experiment design and image acquisition. **Courtney N. Gleason:** Principal investigator of Emory Orthopedics Research Pilot grant. Performed logistical organization of experiment design. **Amanda Blackmon:** Facilitated subject recruitment. **Emma Faulkner:** Facilitated subject recruitment. **Damian Dyckman:** Provided expert guidance on content related to this study's focus. **Monica B. Umpierrez:** Provided expert guidance on content related to this study's focus. **Philip K.W. Wong:** Provided expert guidance on content related to this study's focus. **Vahid Khalilzad Sharghi:** Provided technology utilized to acquire imaging and protocol guidance. **Pan Su:** Provided technology utilized to acquire imaging and protocol guidance. **David A. Reiter:** Principal investigator of NIH R21AR080862 grant. Performed experimental design and image acquisition, data analysis, and manuscript writing. All authors have contributed to critically revising the draft and have approved this final submitted manuscript.

Acknowledgments

This study was supported in part by an Emory Orthopedics Research Pilot grant, Emory Radiology and Imaging Sciences Pilot grant, and National Institutes of Health (NIH) R21AR080869. This manuscript is the result of funding in part by the NIH. It is subject to the NIH Public Access Policy. Through acceptance of this federal funding, NIH has been given the right to make this manuscript publicly available in PubMed Central upon the Official Date of Publication, as defined by NIH.

Conflicts of Interest

The authors declare no conflicts of interest.

STROBE Statement

The authors have prepared and revised the manuscript according to the STROBE statement for cohort studies.

References

1. X. Gao, D. Xu, F. Li, J. S. Baker, J. Li, and Y. Gu, "Biomechanical Analysis of Latin Dancers' Lower Limb During Normal Walking," *Bioengineering (Basel, Switzerland)* 10, no. 10 (2023): 1128, https://doi.org/10.3390/bioengineering10101128.

2. K. L. A. Moore, A. M. R., and A. F. Dalley, *Essential Clinical Anatomy*, 4th ed. (Lippincott Williams & Wilkins, 2015).

3. G. D. Fullerton and A. Rahal, "Collagen Structure: The Molecular Source of the Tendon Magic Angle Effect," *Journal of Magnetic Resonance Imaging* 25, no. 2 (2007): 345–361, https://doi.org/10.1002/jmri.20808.

4. J. Poszepczyński, M. Pietrusiński, M. Borowiec, and M. Edward Domżalski, "Assessment of fibrillin-2 and Elastin Gene Polymorphisms in Patients With a Traumatic Achilles Tendon Rupture: Is Achilles Tendon Rupture a Genetic Disease?," *Acta Orthopaedica et Traumatologica Turcica* 57, no. 2 (2023): 73–77, https://doi.org/10.5152/j.aott.2023.22024.

5. L. E. Eisner, R. Rosario, N. Andarawis-Puri, and E. M. Arruda, "The Role of the Non-Collagenous Extracellular Matrix in Tendon and Ligament Mechanical Behavior: A Review," *Journal of Biomechanical Engineering* 144, no. 5 (2022): 050801, https://doi.org/10.1115/1.4053086.

6. N. Taye, S. Z. Karoulias, and D. Hubmacher, "The 'Other' 15-40%: The Role of Non-Collagenous Extracellular Matrix Proteins and Minor Collagens in Tendon," *Journal of Orthopaedic Research* 38, no. 1 (2020): 23–35, https://doi.org/10.1002/jor.24440.

7. C. T. Thorpe, H. L. Birch, P. D. Clegg, and H. R. C. Screen, "The Role of the Non-Collagenous Matrix in Tendon Function," *International Journal of Experimental Pathology* 94, no. 4 (2013): 248–259, https://doi.org/10.1111/iep.12027.

8. G. H. Filho, J. Du, B. C. Pak, et al., "Quantitative Characterization of the Achilles Tendon in Cadaveric Specimens: T1 and T2*Measurements Using Ultrashort-TE MRI At 3 T," *American Journal of Roentgenology* 192, no. 3 (2009): W117–W124, https://doi.org/10.2214/ajr.07.3990.

9. V. Juras, S. Zbyn, C. Pressl, et al., "Regional Variations ofT2* in Healthy and Pathologic Achilles Tendon In Vivo at 7 Tesla: Preliminary Results," *Magnetic Resonance in Medicine* 68, no. 5 (2012): 1607–1613, https://doi.org/10.1002/mrm.24136.

10. M. F. Joseph, K. Histen, J. Arntsen, et al., "Achilles Tendon Adaptation During Transition to a Minimalist Running Style," *Journal of Sport Rehabilitation* 26, no. 2 (2017): 165–170, https://doi.org/10.1123/jsr.2016-0007.

11. A. Turrina, M. A. Martínez-González, and C. Stecco, "The Muscular Force Transmission System: Role of the Intramuscular Connective Tissue," *Journal of Bodywork and Movement Therapies* 17, no. 1 (2013): 95–102, https://doi.org/10.1016/j.jbmt.2012.06.001.

12. M. A. R. Anjum, F. M. Gonzalez, A. Swain, et al., "Multi-Component Relaxation Modelling in Human Achilles Tendon: Quantifying Chemical Shift Information in Ultra-Short Echo Time Imaging," *Magnetic Resonance in Medicine* 86, no. 1 (2021): 415–428, https://doi.org/10.1002/mrm.28686.

13. A. L. Swain, J., M. R. Anjum, et al. *HR-MAS 1H-NMR Investigations of Ovine Achilles Tendon and Rat Rotator Cuff Tendon* (International Society For Magnetic Resonance In Medicine, Virtual, 2021).

14. T. G. Baumer, L. Davis, J. Dischler, et al., "Shear Wave Elastography of the Supraspinatus Muscle and Tendon: Repeatability and Preliminary Findings," *Journal of Biomechanics* 53 (2017): 201–204, https://doi.org/10.1016/j.jbiomech.2017.01.008.

15. T. G. Baumer, J. Dischler, L. Davis, et al., "Effects of Age and Pathology on Shear Wave Speed of the Human Rotator Cuff," *Journal of Orthopaedic Research* 36, no. 1 (2018): 282–288, https://doi.org/10.1002/jor.23641.

16. W. A. Berrigan, K. Cipriano, K. A. Easley, and K. Mautner, "Quantifying Mechanical Properties of the Patellar and Achilles Tendons Using Ultrasound Shear Wave Elastography: A Pilot Study," *Diagnostics* 15, no. 7 (2025): 879, https://www.mdpi.com/2075-4418/15/7/879.

17. T. Dirrichs, V. Quack, M. Gatz, M. Tingart, C. K. Kuhl, and S. Schrading, "Shear Wave Elastography (SWE) for the Evaluation of Patients With Tendinopathies," *Academic Radiology* 23, no. 10 (2016): 1204–1213, https://doi.org/10.1016/j.acra.2016.05.012.

18. T. Dirrichs, V. Quack, M. Gatz, et al., "Shear Wave Elastography (SWE) for Monitoring of Treatment of Tendinopathies," *Academic Radiology* 25, no. 3 (2018): 265–272, https://doi.org/10.1016/j.acra.2017.09.011.

19. T. Dirrichs, S. Schrading, M. Gatz, M. Tingart, C. K. Kuhl, and V. Quack, "Shear Wave Elastography (SWE) of Asymptomatic Achilles Tendons: A Comparison Between Semiprofessional Athletes and the Nonathletic General Population," *Academic Radiology* 26, no. 10 (2019): 1345–1351, https://doi.org/10.1016/j.acra.2018.12.014.

20. M. S. Taljanovic, L. H. Gimber, G. W. Becker, et al., "Shear-Wave Elastography: Basic Physics and Musculoskeletal Applications," *Radiographics* 37, no. 3 (2017): 855–870, https://doi.org/10.1148/rg.2017160116.

21. A. J. Bayliss, A. M. Weatherholt, T. T. Crandall, et al., "Achilles Tendon Material Properties Are Greater in the Jump Leg of Jumping Athletes," *Journal of musculoskeletal & neuronal interactions* 16, no. 2 (2016): 105–112.

22. C. Anker-Petersen, B. Juul-Kristensen, J. Antflick, et al., "Six Weeks of Intensive Rehearsals for the Swan Lake Ballet Shows Ultrasound Tissue Characterization Changes of the Achilles Tendons in Dancers," *Scandinavian Journal of Medicine & Science in Sports* 31, no. 11 (2021): 2133–2143, https://doi.org/10.1111/sms.14034.

23. F. M. Gonzalez, C. N. Gleason, A. Tran, et al., "Differences in Achilles Tendon Mechanical Properties Between Professional Ballet Dancers and Collegiate Athletes Utilizing Shear Wave Elastography," *Skeletal Radiology* 53, no. 7 (2024): 1381–1388, https://doi.org/10.1007/s00256-024-04564-z.

24. T. Halasi, Á. Kynsburg, A. Tállay, and I. Berkes, "Development of a New Activity Score for the Evaluation of Ankle Instability," *American Journal of Sports Medicine* 32, no. 4 (2004): 899–908, https://doi.org/10.1177/0363546503262181.

25. S. Aubry, J. R. Risson, A. Kastler, et al., "Biomechanical Properties of the Calcaneal Tendon In Vivo Assessed by Transient Shear Wave Elastography," *Skeletal Radiology* 42, no. 8 (2013): 1143–1150, https://doi.org/10.1007/s00256-013-1649-9.

26. K. W. Barfod, A. F. Riecke, A. Boesen, et al., "Validation of a Novel Ultrasound Measurement of Achilles Tendon Length," *Knee Surgery, Sports Traumatology, Arthroscopy* 23, no. 11 (2015): 3398–3406, https://doi.org/10.1007/s00167-014-3175-2.

27. F. M. Gonzalez, C. A. Gleason, K. S. Lee, et al., "Shear Wave Elastography Assessment and Comparison Study of the Achilles Tendons in Optimally Conditioned Asymptomatic Young Collegiate Athletes," *Skeletal Radiology* 50, no. 12 (2021): 2381–2392, https://doi.org/10.1007/s00256-021-03798-5.

28. J. Zuo, E. Saadat, A. Romero, et al., "Assessment of Intervertebral Disc Degeneration With Magnetic Resonance Single-Voxel Spectroscopy," *Magnetic Resonance in Medicine* 62, no. 5 (2009): 1140–1146, https://doi.org/10.1002/mrm.22093.

29. A. Svärd, M. Hammerman, and P. Eliasson, "Elastin Levels Are Higher in Healing Tendons Than in Intact Tendons and Influence Tissue Compliance," *FASEB Journal* 34, no. 10 (2020): 13409–13418, https://doi.org/10.1096/fj.202001255R.

30. Z. M. Beach, C. A. Nuss, S. N. Weiss, and L. J. Soslowsky, "Neonatal Achilles Tendon Microstructure Is Negatively Impacted by Decorin and Biglycan Knockdown After Injury and During Development," *Annals of Biomedical Engineering* 52, no. 3 (2024): 657–670, https://doi.org/10.1007/s10439-023-03414-8.

31. P. S. Robinson, T. F. Huang, E. Kazam, R. V. Iozzo, D. E. Birk, and L. J. Soslowsky, "Influence of Decorin and Biglycan on Mechanical Properties of Multiple Tendons in Knockout Mice," *Journal of Biomechanical Engineering* 127, no. 1 (2005): 181–185, https://doi.org/10.1115/1.1835363.

32. K. A. Robinson, M. Sun, C. E. Barnum, et al., "Decorin and Biglycan Are Necessary for Maintaining Collagen Fibril Structure, Fiber Realignment, and Mechanical Properties of Mature Tendons," *Matrix Biology* 64 (2017): 81–93, https://doi.org/10.1016/j.matbio.2017.08.004.

33. T. Watanabe, Y. Imamura, D. Suzuki, et al., "Concerted and Adaptive Alignment of Decorin Dermatan Sulfate Filaments in the Graded Organization of Collagen Fibrils in the Equine Superficial Digital Flexor Tendon," *Journal of Anatomy* 220, no. 2 (2012): 156–163, https://doi.org/10.1111/j.1469-7580.2011.01456.x.

34. T. Guo, Y. Song, J. Tong, et al., "Collagen Degradation Assessment With an In Vitro Rotator Cuff Tendinopathy Model Using Multiparametric Ultrashort-TE Magnetization Transfer (UTE-MT) Imaging," *Magnetic Resonance in Medicine* 92, no. 4 (2024): 1658–1669, https://doi.org/10.1002/mrm.30144.

35. B. Chen, X. Cheng, E. W. Dorthe, et al., "Evaluation of Normal Cadaveric Achilles Tendon and Enthesis With Ultrashort Echo Time (UTE) Magnetic Resonance Imaging and Indentation Testing," *NMR in Biomedicine* 32, no. 1 (2019): e4034, https://doi.org/10.1002/nbm.4034.

Supporting Information

Additional supporting information can be found online in the Supporting Information section.
Table S1. UTE and SWE measurements in the AT reported as mean ± standard deviation for both non-dancer and dancer groups. **Table S2.** Non-dancer and dancer cohort demographics, UTE data, and SWE measurements.